Bull. Inst. Chem. Res., Kyoto Univ., Vol. 67, No. 2, 1989

TEM Studies on Solution-Grown Crystals of Poly(aryl-ether-ether-ketone) (PEEK)

Masaki TSUJI*, Hidetoshi KAWAMURA**, Akiyoshi KAWAGUCHI*, and Ken-ichi KATAYAMA*

Received June 3, 1989

The morphology of poly(aryl-ether-ether-ketone) [PEEK] crystals grown isothermally from the dilute solution was discussed on the basis of the results by transmission electron microscopy [TEM]. Two typical morphologies were observed: one is a coarse spherulite the constituents of which are seemingly fibrillar but narrow lamellar crystals, and the other is a thick spherulite made up of rather broad lamellae. An intermediate between these two morphologies was also observed. The growth direction of the lamellar crystals corresponded to the b-axis of PEEK crystal lattice, and orientation distribution of crystallites around this axis was confirmed. Such a lamellar crystal exhibited frequent branching and gradual narrowing in width toward the tip of the crystal.

The total end-point dose, namely an electron dose needed for complete destruction of crystallinity, was measured for the PEEK crystal at ~0.1 coulomb/cm^2 for 200 kV electrons at room temperature. This value indicates that PEEK is one of radiation less-sensitive polymers and tough against electron irradiation enough to take a high-resolution TEM image. High-resolution images with the resolution limit of 0.296 nm corresponding to the (020) spacing were successfully obtained, one of which clearly shows the small-angle grain boundary caused by successive edge-dislocations in the ab-plane projection, i.e., in the projection along the molecular stem axis. Lamella branching/narrowing and mutual misorientation of adjoining crystallites were attributed partly to this type of partial edge-dislocation with the probable Burgers vector of (1/2) [100].

KEY WORDS: Poly(aryl-ether-ether-ketone)/ PEEK/ Morphology/ Electron microscopy/ Solution-grown crystal/ High-resolution image/ Dislocation/ Grain boundary/

INTRODUCTION

Poly(aryl-ether-ether-ketone) [PEEK]

$$(\phi\text{-O-}\phi\text{-O-}\phi\text{-CO-})_n$$

with all linkages at the paraposition is one of rigid-chain semicrystalline ploymers with high thermal stability, excellent registance to chemicals and high mechanical strength. Its melting and glass transition temperatures were reported as 335°C and 144°C, respectively[1], and this polymer is not subject to thermal oxidative degradation up to 400°C[2]. Owing to the melt-processibility in addition to the properties mentioned above, PEEK is expected as a high-performance engineering plastics, especially as a matrix resin for advanced composites[3,4]. Thus there have been

* 辻 正樹, 河口昭義, 片山健一 : Laboratory of Polymer Crystals, Institute for Chemical Research, Kyoto University, Uji, Kyoto-fu, 611.

** 河村英俊 : On leave from Tokuyama Soda Co., Ltd., 1-1, Harumi-cho, Tokuyama, Yamaguchi-ken, 745.

published many papers so far, for example concerning the crystal structure analysis by the X-ray diffraction method[1,3,5-8], the thermal behavior[2,4,9-11] and mechanical properties[12-14]. Crystallization and morphology of PEEK from the melt were studied extensively[15-20], and it was reported that PEEK is closely analogous to poly (ethylene terephthalate) in the crystallization behavior[15]. Recently, the structure information obtained by neutron scattering[21] and the intrinsic birefringence[22] of PEEK were also reported.

Transmission electron microscopy [TEM] of PEEK was first reported by Lovinger and Davis for its solution-grown crystals[23,24]. In TEM studies on melt-crystallized PEEK, thin films cast from solutions[16], thin sections[17] and two-stage replicas of the specimen treated by permanganic etching[19,20] were used. Recently, Waddon *et al.*[25] carried out a comparative study on PEEK, poly(aryl-ether-ketone) [PEK] and poly(*p*-phenylene sulphide) [PPS] because these polymers have similar crystal structures one another. Judging from the low crystallinity[15] and a rather small crystallite-size[13] of PEEK, many defects are expected to exist in the PEEK crystal. These defects should have a great influence on mechanical properties of PEEK products such as fibers. In order to observe such a defect directly and to define molecular arrangement in the vicinity of the defect, high-resolution TEM is the best and unique method[26], but no studies have been done yet on high-resolution TEM of PEEK whereas PEK[27], which is of the same family as PEEK and has higher crystallinity than PEEK[1], was studied by this method. The nautre of the defects and the orientational relationship between adjoining misoreinted crystallites in solution-grown crystals are anticipated to be inherently the same as those in bulk materials. In this paper, hence, the solution-grown crystals of PEEK are examined by high-resolution TEM. First of all, the morphological features of PEEK solution-grown crystals are discussed, and then the preliminary results in high-resolution TEM are shown.

EXPERIMENTAL

Commercial molding chips of PEEK were disolved in α-chloronaphthalene at its boiling point. Though the molecular weight of the PEEK sample is not known, it is presumed as $\overline{M}w=20,000\sim35,000$ because the sample came from the same source (ICI Plastics Ltd.) as that used by Lovinger and Davis[24]. The 0.02 wt% solution was transferred into an oil bath, and then PEEK crystals were grown isothermally at 208.6 ($\pm$0.6)°C under a nitrogen atmosphere for two days. The solution was then cooled down to room temperature. A drop of the crystal suspension was transferred onto a carbon support-film deposited on a copper specimen grid. For high-resolution TEM, a very thin carbon support-film ($<$10 nm in thickness) on an Ag- or Au-coated Triafol "microgrid" was used. The specimen thus prepared was dried in a vacuum evaporator ($\leqq 10^{-4}$Pa). For morphological observation, it was shadowed with Pt-Pd at a shadow angle of $\tan^{-1}(1/4)$. To measure lattice spacings, PEEK crystals were deposited on an aluminum support-film. TEM of PEEK crystals was performed using a JEOL JEM-200CS equipped with a Minimum Dose System[28]

and a thermionic LaB_6 electron source. The microscope was operated at 200kV and its spherical aberration coefficient C_s is 2.8 mm. All the electron diffraction patterns and images were recorded on Mitsubishi electron microscope films [MEM] which were developed in the full strength of the Gekkol developer (Mitsubishi Paper Mills Ltd.) at 20°C for 5 min. The electron beam current was measured with a picoammeter which was connected to the Faraday cup set in the viewing chamber of the microscope.

RESULTS AND DISCUSSION

1) Morphologies of PEEK solution-grown crystals

Solution-grown crystals of PEEK are shown in Fig. 1, where two different morphologies are recognized. One of them, which is shown in Fig. 1-a, is a coarse spherulite whose textural constituents are seemingly "fibrillar" but very narrow lamellar crystals of 20～40 nm in width and 10～15 nm in thickness. Here the thickness was estimated from the shadow length and angle. This morphology is almost identical to that reported by Lovinger and Davis[24]. The other morphology (demonstrated in Fig. 1-b) corresponds to a thick spherulite, which has a sheaf-like appearance. As deduced from the long shadow, such a spherulite still preserves approximately its original three-dimensional form after the depostion on a carbon support-film. The overall thickness (height) is estimated at 3～4μm from the shadow length and is smaller than its lateral size (about 7 μm×9 μm). This means that

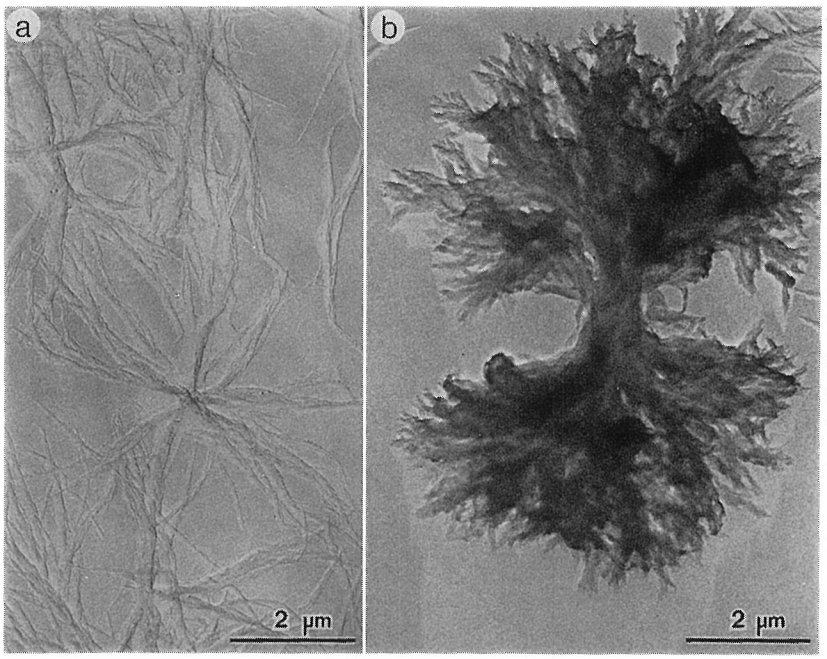

Fig. 1. Typical molphologies of PEEK crystals grown isothermally at 208.6°C from the 0.02wt% solution in α-chrolonaphthalene (shadowed with Pt-Pd).
a) Seemingly fibrillar but narrow lamellar crystals. They form a coarse spherulite.
b) Thick spherulite with a sheaf-like appearance. Its constituents are lamellae.

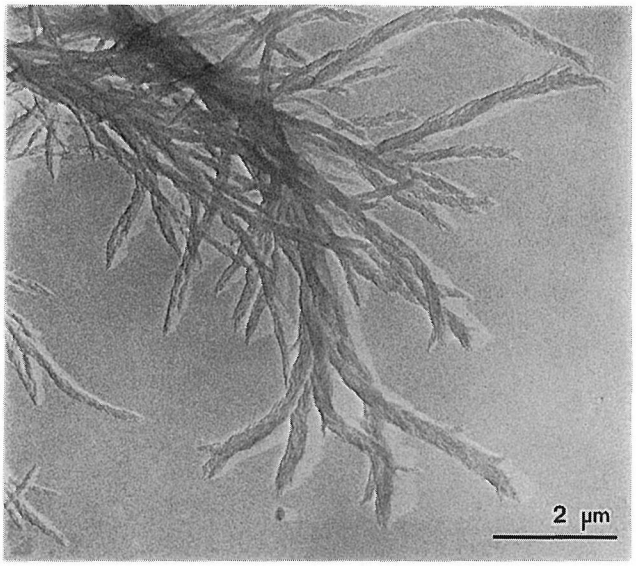

Fig. 2. Molphology observed occasionally together with those in Fig. 1, showing an intermediate between fibrillar (Fig. 1-a) and spherulitic (Fig. 1-b) morphologies. The broad fibrillar lamellae in this figure are very similar to the constituents of the thick spherulite in Fig. 1-b.

the spherulite was pressed down on the support-film. The thickness of constituent lamellae of the spherulite is about 10 nm from the shadow length. This thickness is practically equal to that of fibrillar lamellae in Fig. 1-a and also to the values reported so far for the PEEK "single crystal" and the constituent lamellae of spherulites[23,24]. At the tip of a lamella in the thick spherulite, however, lamellar thickness is less than 10 nm. The width of the lamellae was not measured because they are piled one upon another, but is possibly much larger than that of seemingly fibrillar crystals in Fig. 1-a. Figure 2 shows an intermediate texture between the thin fibrils in Fig. 1-a and the thick spherulite in Fig. 1-b. The structural units of this texture are lamellae and their width is several times greater than that of fibrillar crystals in Fig. 1-a, but they are not organized enough to make up a well-defined spherulite as in Fig. 1-b. The thickness of lamellae in Fig. 2 is nearly the same as that of fibrils and lamellae in Fig. 1. It seems that narrower lamellae in Fig. 1-a were grown during subsequent cooling of the solution to room temperature, as proposed by Lovinger and Davis[24]. They also proposed that the spherulite showing the sheaf-like growth (Fig. 1-b) was homogeneously nucleated, while the spherulite as shown in Fig. 1-a was heterogeneously nucleated and its constituent narrow lamellae were radially grown straight from its center. At higher crystallization temperature, say at 220°C, isolated single crystal lamellae were observed by them[23,24]. In our experiment, however, such a morphology is not obtained at present. In addition, they proposed the "microfaceting" of the single crystal on a scale less than about 100 nm. Here the word, microfaceting, means that the small crystals of PEEK are bounded with (100), (010) and {110} planes. In Figs. 1 and 2, microfaceting is not recognized.

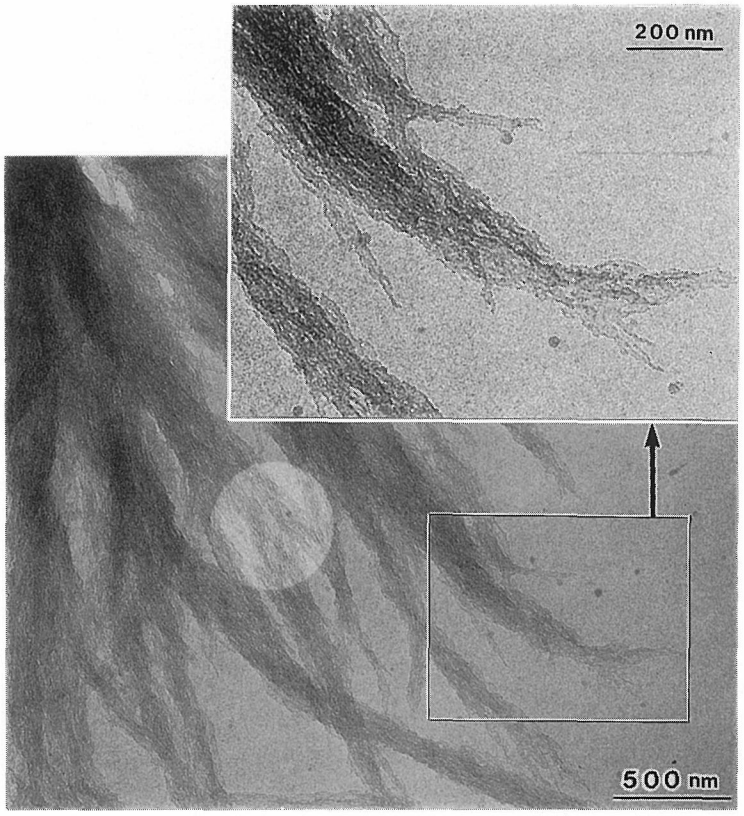

Fig. 3. Defocused image of PEEK solution-grown crystals. This image was taken at a few μm underfocus, and it reveals irregular-shaped microcrystals comprising a fibrillar lamella by defocus contrast[39]. The inset ia a highly enlarged photograph of the corresponding rectangular area. Encircled is the area to give the electron diffraction pattern of Fig. 4. Fibrillar axis, namely the growth direction, corresponds to the b-axis.

Figure 3 shows the fibrillar crystals of PEEK, which correspond to Fig. 1-a and are not shadowed. This micrograph was taken at a rather large amount of defocus (a few μm underfocus). Each fibrillar crystal, in this figure, exhibits frequent branching and gradual narrowing in width toward the tip of the crystal, as also recognized in Fig. 1-a. The inset of Fig. 3, the highly enlarged micrograph of the corresponding rectangular area, clearly reveals that the fibrillar crystal is apparently composed of many irregular-shaped microcrystals of several tens of nm in width[24], and again microfaceting is not observed. Figure 4 shows the selected-area electron diffraction pattern from the encircled area in Fig. 3. The area is about 500 nm in diameter. The directional relationship between Fig. 3 and 4 shows that as already proposed[23-25], the fibrillar axis corresponds to the b-axis of the PEEK crystal lattice: the crystal structure of PEEK was analyzed by Shimizu *et al.*[7] as

orthorhombic [*Pbcn*], a=0.780 nm, b=0.592 nm, c(chain axis)=1.000 nm.

According to their result, the main-chain conformation is planar zigzag and the

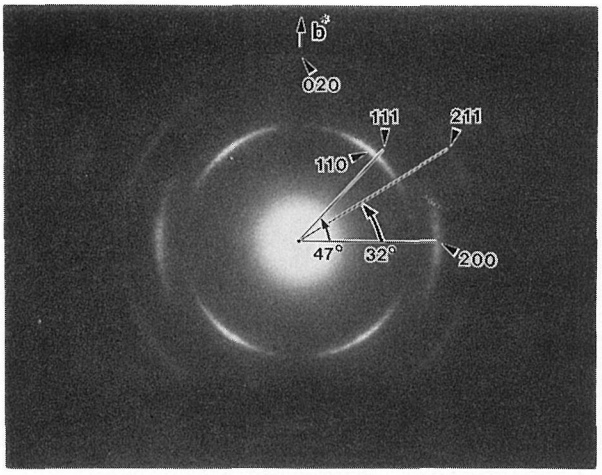

Fig. 4. Selected-area electron diffraction pattern of PEEK solution-grown crystals (from the encircled area in Fig.3) This pattern was well indexed using the unit cell dimensions proposed by Shimizu *et al*[7]. The angles between the lines drawn from the origin to the centers of 200 and *h*11 reflections are in good agreement with those calculated from the unit cell dimensions, assuming the orientation distribution of the crystallites around the *b*-axis (calculated angles are 46.1° for 111 and 31.5° for 211).

zigzag planes of all molecular stems are parallel to the b-axis, as proposed first by Dawson *et al.*[1] and also by others[3,5,6,8]. The planes of the phenylene rings are alternately inclined at $\pm 37°$ with respect to the (100) plane[7]. The c dimension of the unit cell corresponds to the length of two aryl units in a fully extended planar conformation and is two-thirds of the chemical repeat of this polymer because of structural disorder and crystallographic equivalence of the ether and carbonyl units[1,5-7]. In Fig. 4, the reflections of 111 and 211 are observed together with fairly strong *hk*0 reflections. Hence most of PEEK molecular stems are oriented normal to the support-film surface, but the rest are not so. From the azimuthal angles of the centers of arced 111 and 211 reflections with respect to the center of the 200 reflection, it is concluded that the orientation distribution was produced by tilting the crystallites around the b-axis, and not around the a-axis. The intensity of 111 is apparently weaker than that of 211 in Fig. 4. The difference in intensity between these two reflections is much greater than that expected from the structure amplitudes for these reflections[7]. Furthermore, 00*l* reflections are not recognized in Fig. 4. These results strongly support the above consideration and allow us to estimate the angular distribution of the crystallites around the b-axis as $\pm 38°$ at most. We already discussed this kind of orientation distribution in detail for PPS solution-grown crystals[29]. The electron diffraction patterns from the thin, peripheral portions of the spherulite shown in Fig. 1-b and those from broad fibrillar crystals shown in Fig. 2 were basically the same as Fig. 4: the growth direction of the constituent crystal lamellae (the radial direction of the spherulite) is in the direction of the b-axis.

2) High-resolution TEM of PEEK solution-grown crystals

The less-sensitivity of PEEK crystals against electron irradiation was first studi-

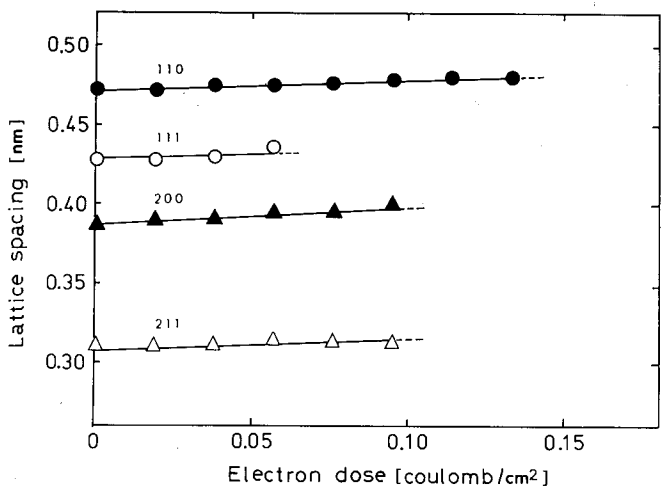

Fig. 5. Variation of lattice spacings of PEEK crystal with 200kV electron irradiation dose at room temperature. The lines for 110, 111 and 211 were drawn according to the result of calculation from the experimental line for 200 and from the unit cell dimensions of unirradiated crystal lattice (● for 110, ○ for 111, ▲ for 200 and △ for 211).

ed quantitatively by Yoda: the c dimension of the crystal lattice is little affected with increasing electron dose[30]. Figure 5 shows the variation of lattice spacings of PEEK crystal with increasing dose of 200 kV electrons at room temperature. All these spacings slightly increase with electron dose while their intensities gradually decrease. In particular, the (200) spacing increases a little faster than the (110) spacing. Though the change in the (020) spacing was not measured at present, this spacing is anticipated to be substantially unchanged. Thus the PEEK crystal lattice is predicted to expand in the direction parallel to the a-axis due to electron irradiation, as is the case of PPS[31]. Figure 5 also shows that the 110 reflection is the most durable against electron irradiation. The electron dose corresponding to complete disappearance of the 110 reflection is, consequently, defined as the total end-point dose [TEPD] of PEEK crystal. As an average from repeated measurements, the TEPD of PEEK crystal was estimated at about 0.1 coulomb/cm^2 for 200 kV electrons at room temperature. Kumar *et al.*[17] reported that the TEPD of PEEK is about 0.03 coulomb/cm^2 for 100 kV electrons. Taking account of the facts that the higher the electron energy, the greater the TEPD and that the TEPD is not always defined by the consistent standard, the difference between these two values may be reasonable. Though it was pointed out that both crosslinking and chain scission take place under electron irradiation[32], the detailed process and mechanism of radiation damage of PEEK crystal are not yet known.

The smallest spacing d [nm] of lattice fringes which are expected to be observable directly on electron micrographs is estimated using the following equation[33]:

$$d = 1.5/0.1\sqrt{0.25N},$$

where N [electrons/nm^2] means the TEPD of the specimen. For PEEK, $N=\sim 0.1$

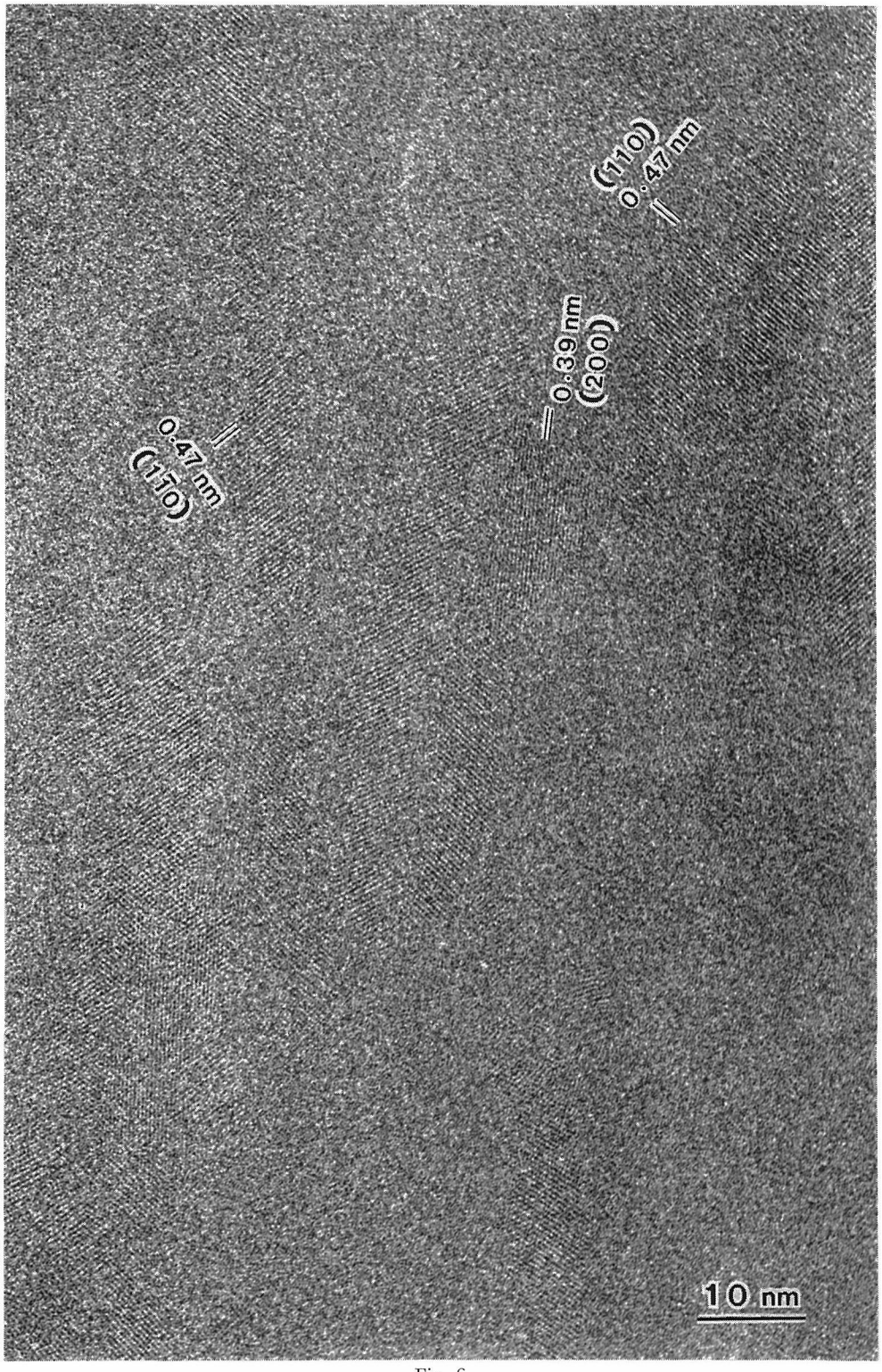

Fig. 6

coulomb/cm^2=~6×10^3 electrons/nm^2. Then d is estimated as 0.39 nm, which is almost the same as the (200) lattice spacing of 0.390 nm and is smaller than the (110) spacing of 0.472 nm. Hence we can fully expect the lattice images of PEEK crystal on which we directly discern the orientation and size of individual crystallites comprising fibrillar and lamellar crystals of PEEK. On the basis of the sensitivity and resolution limit of the photographic films (MEM)[34] and the TEPD of PEEK, the photographing condition for high-resolution TEM of PEEK crystals was set: electron optical magnification=100,000; electron beam current on specimen= 0.09 A/cm^2; exposure time=1 sec; total dose for image recording=0.09 coulomb/cm^2. Photographing of thin "fibrillar" crystals shown in Fig. 1-a was mainly tried, because they give a well-balanced *hk*0-pattern in electron diffraction. On the other hand, the specimens with a thick spherulitic texutre in Fig. 1-b sometimes cause specimen drift during photographing because they are in poor contact with the support film, when they are damaged accompanying shrinkage due to a strong electron current for high-magnification imaging.

Figure 6 shows an example of high-resolution electron micrographs thus obtained from PEEK solution-grown crystals. In this figure, the fibrillar axis is vertical and (200) and/or {110} lattice fringes are directly observed here and there. In particular, some are curved, which implies lattice distortion. The corresponding optical diffractogram from the ~8 mmϕ area in the original negative (~70 nm in diameter on the specimen) is shown in Fig. 7. This diffractogram shows 200, 110, 1$\bar{1}$0, and 020 (0.296 nm in spacing) reflections, and a weak 211 reflection (0.310 nm) is also recognized (indicated by white arrows in Fig. 7). All the *hk*0 reflections are slightly arced, which indicates misorientation. When the area illuminated by a laser beam is reudced to 3 mmϕ (~30 nmϕ on the specimen) in taking an optical diffracto-

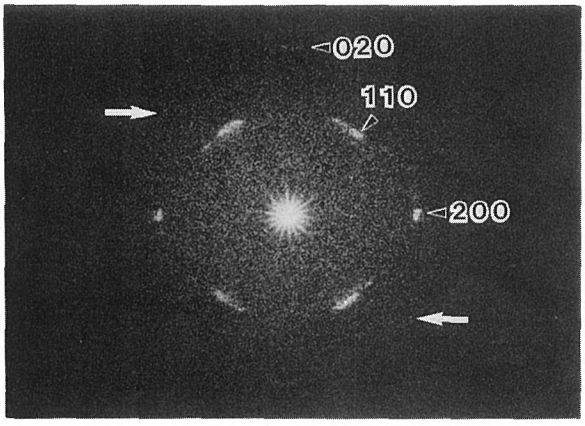

Fig. 7. Optical diffractogram from the ~8mmϕ area in the original negative (~70nmϕ on the specimen), corresponding to Fig. 6. White arrows indicate a weak 211 reflection.

Fig. 6. An example of high-resolution TEM images of PEEK solution-grown crystals. Fibrillar axis is vertical, but the growth direction is unknown (upward or downward). (200) and/or {110} lattice fringes are observable here and there.

gram, a single-crystal-like un-arced $hk0$-pattern was obtained. This means that the size of a coherent crystallite is the order of about 30 nm in diameter. The careful inspection of Fig. 6 actually reveals that the area, in which lattice fringes are coherently aligned, is elongated along the fibrillar axis, namely the b-axis, and its size was measured directly at about 10 nm along the a-axis and about 20 to 60 nm along the b-axis. From the morphological observation of PEEK single crystal, Lovinger and Davis also reported the narrow crystal habit (elonagted in the direction parallel to the b-axis)[24]. In Fig. 6, microfaceting is not recognized for the crystallites defined by the observable lattice fringes. It seems, however, that the side surface of each elongated crystallite is basically the (100) plane.

Figure 8-a is a highly enlarged micrograph, showing an irregular structure in the PEEK crystal. Each dark spot in this figure corresponds to a PEEK molecular chain stem viewed along the stem axis. Some clear spots are indicated by small arrows. Inspection in the direction indicated by the thick arrow marked at the bottom of the figure (see also Fig. 8-b) reveals that the (200) lattice fringes are curved: a set of fringes in the left-hand side are curved to the left and the other set in the

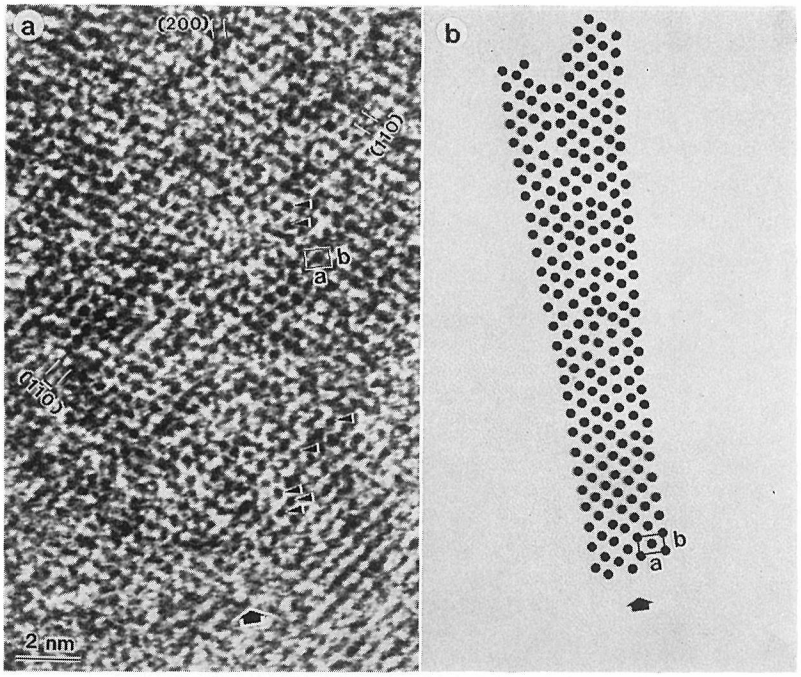

Fig. 8. a) Highly enlarged TEM image of PEEK solution-grown crystal, showing a small-angle grain boundary caused by successive edge-dislocations. The growth direction of the fibrillar crystals is vertical (upward or downward). Dark spots appear in the area in which (200), (110) and (1$\bar{1}$0) fringes are observable together: some clear spots are indicated by small arrows. Each spot corresponds to the PEEK molecular stem projected on the ab-plane along the stem axis (the c-axis). a=0.780 nm, b=0.592 nm[7].
b) Schematic representation of molecular arrangement in the vicinity of the boundary in (a). Each solid circle represents a molecular stem of PEEK viewed along its axis.

righ-thand side to the right. The orientation of crystal lattice in the left-hand side is different from that in the right-hand side, in the upper half of the figure, which fact means the misorientation. Extra fringes are recognized between these two sets of fringes. This figure demonstrates an example of small-angle grain boundary[35], which is in conjunction with successive edge-dislocations. Figure 8-b shows schematic representation of molecular packing in the vicinity of boundary: the arrangement of dark spots in Fig. 8-a was straightfowardly traced to make Fig. 8-b with solid circles. This type of dislocation is considered to be a partial one with the probable Burgers vector of (1/2) [100]. This dislocation should be accompanied by a stacking fault. For the crystal lamella of PEEK growing upward to the top of Fig. 8-a, lamella branching caused by this type of dislocation may take place. On the other hand, for the crystal growing downward, this type of dislocation may be an origin of narrowing in lamella width. Thus it is deduced that this type of edge dislocation is one of origins of lamella branching/narrowing as well as a cause of mutual misorientation of adjoining crystallites.

As the lamellar thickness of PEEK increases with increasing crystallization and annealing temperatures[4,11,15] and the plastic deformation from lamellar to fibrillar structures takes place in stretching lamellae in the direction parallel to the lamella surface[36], it should be concluded that PEEK crystallizes in a chain-folded macroconformation. The PEEK crystal seems to have such a type of partial edge-dislocation with an extra (200) plane as that shown in Fig. 8. Lovinger and Davis have already proposed that the (200) planes are more susceptible to cleavage and therefore such susceptibility contributes to the restricted width, fragmentation and mutual misorientation[24]. According to their proposal, Waddon *et al.* suggested that the fold plane is parallel to the long dimension, namely in the direction of the b-axis of the crystal[25]. Putting our and their accounts together, the (100) fold seems to be the most probable of all possibilities in PEEK crystals.

CONCLUDING REMARKS

The appearance of $h11$ reflections on the electron diffraction pattern of PEEK solution-grown crystals was well explained by the orientation distribution of the crystallites around the b-axis, namely the "fibrillar" axis. The distortion responsible for the orientation distribution is approximated by alternate twisting[37] of the "fibrillar" crystal in a non-periodic manner.

The PEEK crystal belongs to a class of less-sensitive polymers against electron irradiation. The TEPD of PEEK crystal was measured at about 0.1 coulomb/cm^2 for 200 kV electrons at room temperature. Consequently PEEK is twice as vulnerable as PPS, but is 14 times more resistant than PE against electron irradiation[29,38]. High-resolution electron micrographs were successfully obtained, on which the crystallite size and the mutual orientation between crystallites were specified and the small-angle grain boundary caused by the accumulated edge-dislocations was identified. At present, the detailed molecular arrangement in the vicinity of the grain bounday is not known because of the poor image quality due to the low signal-

to-noise ratio. Computer image-processing is one of possibilities to improve the signal-to-noise ratio. Such an investigation is in progress.

ACKNOWLEDGEMENT

The authors wish to acknowledge Prof. Dr. J. Petermann, Technical University Hamburg-Harburg, FRG, for the supply of PEEK chips.

REFERENCES

(1) P.C. Dawson and D.J. Blundell, *Polymer,* **21,** 577 (1980).
(2) S.-S. Chang, *Polym. Commun.,* **29,** 138 (1988).
(3) N.T. Wakelyn, *Polym. Commun.,* **25,** 306 (1984).
(4) Y. Lee and R.S. Porter, *Macromolecules,* **20,** 1336 (1987).
(5) D.R. Rueda, F. Ania, A. Richardson, I.M. Ward and F.J. Balta Calleja, *Polym. Commun.,* **24,** 258 (1983).
(6) J.N. Hay, D.J. Kemmish, J.I. Langford and A.I.M. Rae, *Polym. Commun.,* **25,** 175 (1984).
(7) J. Shimizu, T. Kikutani, Y. Ookoshi and A. Takaku, *Sen-i Gakkaishi,* **41,** T-461 (1985).
(8) A.V. Fratini, E.M. Cross, R.B. Whitaker and W.W. Adams, *Polymer,* **27,** 861 (1986).
(9) S.Z.D. Cheng, M.-Y. Cao and B. Wunderlich, *Macromolecules,* **19,** 1868 (1986).
(10) M. Day, T. Suprunchuk, J.D. Cooney and D.M. Wiles, *J. Appl. Polym. Sci.,* **36,** 1097 (1988).
(11) Y. Lee, R.S. Porter and J.S. Lin, *Macromolecules,* **22,** 1756 (1989).
(12) T. Kunugi, A. Mizushima and T. Hayakawa, *Polym. Commun.,* **27,** 175 (1986).
(13) J. Shimizu, T. Kikutani, Y. Ookoshi and A. Takaku, *Sen-i Gakkaishi,* **43,** 507 (1987).
(14) Y. Lee, J.-M. Lefebvre and R.S. Porter, *J. Polym. Sci.: B: Polym. Phys.,* **26,** 795 (1988).
(15) D.J. Blundell and B.N. Osborn, *Polymer,* **24,** 953 (1983).
(16) A.J. Lovinger and D.D. Davis, *J. Appl. Phys.,* **58,** 2843 (1985).
(17) S. Kumar, D.P. Anderson and W.W. Adams, *Polymer,* **27,** 329 (1986).
(18) H.X. Nguyen and H. Ishida, *J. Polym. Sci.: B: Polym. Phys.,* **24,** 1079 (1986).
(19) R.H. Olley, D.C. Bassett and D.J. Blundell, *Polymer,* **27,** 344 (1986).
(20) D.C. Bassett, R.H. Olley and I.A.M. Al Raheil, *Polymer,* **29,** 1745 (1988).
(21) B. Hammouda, D.G. Reichel and C.J. Wolf, *J. Macromol. Sci.-Phys.,* **B27,** 445 (1988).
(22) M. Cakmak, *J. Polym. Sci.:C:Polym. Letters,* **27,** 119 (1989).
(23) A.J. Lovinger and D.D. Davis, *Polym. Commun.,* **26,** 322 (1985).
(24) A.J. Lovinger and D.D. Davis, *Macromolecules,* **19,** 1861 (1986).
(25) A.J. Waddon, M.J. Hill, A. Keller and D.J. Blundell, *J. Mater. Sci.,* **22,** 1773 (1987).
(26) S. Isoda, M. Tsuji, M. Ohara, A. Kawaguchi and K. Katayama, *Makromol. Chem., Rapid Commun.,* **4,** 141 (1983).
(27) D. Yan, L. Ge, X. Jin and E. Zhou, Proc. IUPAC 32-nd Int. Symp. Macromol. (Kyoto), p. 725 (1988).
(28) Y. Fujiyoshi, T. Kobayashi, K. Ishizuka, N. Uyeda, Y. Ishida and Y. Harada, *Ultramicrosc.,* **5,** 459 (1980).
(29) A. Uemura, S. Isoda, M. Tsuji, M. Ohara, A. Kawaguchi and K. Katayama, *Bull. Inst. Chem. Res., Kyoto Univ.,* **64,** 66 (1986).
(30) O. Yoda, Polym. Commun., **26,** 16 (1985).
(31) A.J. Lovinger, F.J. Padden Jr. and D.D. Davis, *Polymer,* **29,** 229 (1988).
(32) T. Sasuga and M. Hagiwara, *Polymer,* **27,** 821 (1986).
(33) M. Tsuji, S. Moriguchi, K.J. Ihn, A. Kawaguchi and K. Katayama, Proc. 11-th Int. Congr. EM, Kyoto, p. 1749 (1986).
(34) M. Tsuji, *Kobunshi Kako,* **35,** 522 (1986)/**35,** 574 (1986).
(35) B. Wunderlich, "Macromolecular Physics", vol. 1, Academic Press, New York, p. 469 (1973).
(36) A. Karbach, *Polym. Commun.,* **28,** 24 (1987).
(37) K. Katayama, S. Isoda, M. Tsuji, M. Ohara and A. Kawaguchi, *Bull. Inst. Chem. Res., Kyoto Univ.,* **62,** 198 (1984).
(38) A. Uemura, M. Tsuji, A. Kawaguchi and K. Katayama, *J. Mater. Sci.,* **23,** 1506 (1988).
(39) J. Petermann and H. Gleiter, *Philos. Mag.,* **31,** 929 (1975).